



# On the escape of cosmic ray leptons and their impact on the background plasma

E. Amato<sup>1,2</sup>, P. Blasi<sup>3</sup>, B. Olmi<sup>1,4</sup>, G. Morlino<sup>1</sup>, C. Evoli<sup>3</sup>, N. Bucciantini<sup>1,2</sup>, R. Aloisio<sup>3</sup>, R. Bandiera<sup>1</sup>, L. Del Zanna<sup>2</sup>, D. Gaggero<sup>5</sup>, and D. Grasso<sup>6</sup>

<sup>1</sup> INAF - Osservatorio Astrofisico di Arcetri, Largo E. Fermi 5, 50125, Firenze, Italy, e-mail: elena.amato@inaf.it

<sup>2</sup> Università degli Studi di Firenze, Via Sansone 1, 50019, Sesto Fiorentino (FI), Italy

<sup>3</sup> Gran Sasso Science Institute, Via M. Jacobucci 2, 67100, L'Aquila, Italy

<sup>4</sup> INAF - Osservatorio Astronomico di Palermo, P.zza del Parlamento 1, 90134, Palermo, Italy

<sup>5</sup> Università di Torino, Dipartimento di Fisica, via P. Giuria 1, 10125, Torino, Italy

<sup>6</sup> INFN, Sezione di Pisa, Largo B. Pontecorvo 3, 56125, Pisa, Italy

Received: 31 December 2021; Accepted: 26 May 2022

**Abstract.** The last decade has seen the emergence of a wealth of observational evidence directly related to the escape of cosmic rays (CRs) from their acceleration sites. In this article we focus on leptonic CRs and in particular on scenarios in which Pulsar Wind Nebulae (PWNe) are identified as the main sources of CR positrons above few tens of GeV. We review recent results from observations of PWNe and the theoretical developments that have followed. We discuss the requirements that direct measurements impose on the properties of the accelerators of cosmic leptons and the constraints provided by the latest X-ray and  $\gamma$ -ray observations on the phenomenon of particle release by PWNe, suggesting a scenario in which, as already claimed for hadronic CRs, also CR leptons can modify the properties of the medium in which they propagate.

**Key words.** Astrophysics - High Energy Astrophysical Phenomena; ISM: cosmic rays; magnetic fields; MHD; Physical processes: particle acceleration; non-thermal radiation

## 1. Introduction

A major discovery brought about by direct cosmic ray (CR) measurements from space is the evidence for a rise with energy of the ratio between the flux of positrons and electrons, the so-called *positron excess* (Adriani et al. 2009; Aguilar et al. 2013, 2019b). This fact was immediately found to challenge the standard paradigm associating CR  $e^+$  with the in-

teractions of hadronic CRs with the interstellar plasma during their propagation through the Galaxy (see e.g. Amato & Blasi 2018; Amato & Casanova 2021 for recent reviews). The large majority of the scientific community took this evidence as suggestive of the need for sources of primary  $e^+$  and the possibility of identifying it as the long awaited signature of dark matter decay or annihilation excited vast interest. However, careful scrutiny makes this

scenario challenging for current dark matter models (Serpico 2012). In addition, it was soon realized that there are excellent astrophysical candidates that can explain a  $e^+$  excess (Blasi & Amato 2011): the magnetospheres of pulsars (PSRs hereafter) are very efficient factories of leptonic anti-matter, producing between  $10^3$  and  $10^6$   $e^+ - e^-$  pairs for each  $e^-$  extracted from the star surface (Amato 2019 and references therein). It is clear then that their contribution to CR  $e^+$  must be correctly accounted for, before quantitatively assessing the existence of an *excess* of non-astrophysical origin.

In fact, the PSR produced leptons are not directly released in the interstellar medium (ISM). They are initially confined within a magnetized nebula, the so-called Pulsar Wind Nebula (PWN), where their spectrum is determined under the action of acceleration, advective transport and losses. The relativistic pairs are only injected in the ISM at late times of the PWN evolution, and important aspects of their release can only be investigated by studying the late evolutionary phases of the host nebulae.

Surprising news on the latter have recently come from observations at Very and Extremely High Energies (VHE and EHE, corresponding to photon energies  $> 100$  GeV and  $> 100$  TeV respectively). Halos of diffuse  $\gamma$ -ray emission, interpreted as Inverse Compton scattering (ICS) of leptons with energies in the tens to hundreds TeV range, were observed by HAWC around the well known PSRs associated with Geminga and Monogem (Abeysekara et al. 2017). Spatially extended emission up to PeV photon energies was detected by LHAASO from a dozen sources, most of which likely associated with PSRs (Cao et al. 2021). Both pieces of information might provide important constraints on the particle release from PWNe, and more generally on the processes that govern the escape of energetic particles from astrophysical sources. Particularly intriguing is the possibility that these observations might be pointing to extended confinement times of particles around sources as a result of the modifications induced on the ambient medium by the escaping particles themselves (López-Coto et al. 2022). Understanding the origin of this

phenomenon is a necessary step to assess its importance for the general framework of CR transport in the Galaxy.

The article is structured as follows. In § 2 we briefly summarize current knowledge and recent results on PWNe, discussing the different stages of their evolution and the relevance of evolved systems for CR physics. In § 3 we review the requirements about the sources of  $e^- - e^+$  in the Galaxy that come from CR lepton measurements at the Earth. In § 4 we discuss recent progress and challenges in our understanding of how  $e^- - e^+$  are released by PWNe in light of X-ray and  $\gamma$ -ray observations. Our conclusions are presented in § 5.

## 2. Pulsar Wind Nebulae

PSRs, highly magnetized, fast spinning neutron stars, born in the majority of core-collapse supernova (SN) explosions, loose most of their rotational energy to the production of a magnetized  $e^- - e^+$  wind (see Amato (2019) for a recent review). In young systems this wind is confined by the surrounding supernova remnant (SNR), which forces its expansion, highly relativistic in the vicinity of the star, to slow down. This happens at a termination shock (TS), where the wind ram pressure is dissipated and converted, with very large efficiency (up to  $\sim 30\%$ , as inferred in the case of Crab, see e.g. Amato & Olmi 2021), into particle acceleration. The accelerated particles then give rise to bright non-thermal nebulae, typically shining through synchrotron and ICS emission in a very broad frequency range, from radio to multi-TeV, and even PeV  $\gamma$ -rays. Multi-wavelength study of the emission allows one to constrain the particle spectrum, which typically shows a broken power-law shape:  $N(E) \propto E^{-\gamma_1}$  for  $E < E_b$  and  $N(E) \propto E^{-\gamma_2}$  for  $E > E_b$ , with a relatively flat spectral index,  $1 < \gamma_1 < 2$  for energies less than  $0.2 \text{ TeV} < E_b < 0.8 \text{ TeV}$  and  $\gamma_2 \approx 2.5$  at higher energies.

These spectral properties are mostly derived from observations of young sources (still in the free expansion phase of the SNR), which are the best studied and characterized in terms of particle content. However, these systems are not the ones to consider when looking for

the sources of the  $e^+$  excess, since here particles are confined within the SNR and cannot be efficiently released into the ISM. The following phases of evolution are more relevant. The free expansion phase ends when the PWN boundary is reached by the SNR reverse shock, travelling from the SN ejecta to the center of the explosion. This interaction might cause a strong compression followed by an enhancement of the emission at almost all wavelengths (see e.g. Torres et al. 2019; Bandiera et al. 2020). The contact discontinuity between the PWN and the ejecta is likely fragmented, possibly favouring the escape of particles. This contribution is still to be taken into account in the synthesis of the CR lepton spectrum, due to the lack of data and reliable physical modeling, which requires investigation of this phase of the PWN evolution through proper, highly challenging, multi-dimensional MHD simulations. Important information might come from the upcoming  $\gamma$ -ray facilities, such as CTA predicted to increase by a factor of  $\sim 10$  the number of detected PWNe, the large majority of which during the late stages of the evolution (Fiori et al. 2022).

A better studied phase is the later evolution, after the PSR leaves its parent SNR. A large fraction of all PSRs is in fact likely to escape the SNR within a few  $\times 10^4$  yr after the SN explosion, due to the high average velocity of the PSR population,  $v_{\text{PSR}} \sim 350$  km/s, (Faucher-Giguère & Kaspi 2006). The PSR wind will then interact directly with the ISM, and since the ISM sound speed ( $c_s \sim 10 - 100$  km/s) is generally much lower than the PSR velocity, this induces the formation of a bow shock. These systems, known as *bow-shock pulsar wind nebulae* (BSPWNe), are characterized by a cometary shape, with the PSR located at the bright head of an elongated tail of plasma, extending in the direction opposite to the PSR motion (Bykov et al. 2017).

Even before the detection of TeV halos and the suggestion of a possible association to the  $e^+$  excess, BSPWNe gained much attention due to the discovery of a variety of intriguing features surrounding an (increasing) number of sources. One sided collimated and elongated jets, almost monochromatic in X-rays,

have been observed to develop in a direction strongly misaligned with respect to the PSR proper motion (Hui & Becker 2007; Pavan et al. 2014; Klingler et al. 2020; de Vries & Romani 2020). Less extended X-ray *prongs* or *whiskers* have been seen to arise close to the BSPWN head (Temim et al. 2015; Klingler et al. 2016; Kargaltsev et al. 2017; Kim et al. 2020).

An early suggestion by Bandiera (2008) was that the powerful misaligned jet observed in the Guitar nebula (Hui & Becker 2007) could be interpreted as due to synchrotron emission of particles with energies of order 50 TeV streaming out of the BSPWN along the ambient ISM magnetic field. An interesting implication of this modeling was that the ISM magnetic field strength in that region has to be in the 40-50  $\mu\text{G}$  range, a factor 10-20 times higher than the average field in the Galaxy. In addition, given the spin-down energy of the Guitar PSR,  $\dot{E} = 1.2 \times 10^{33}$  erg/s, the emitting particles have an energy extremely close to the maximum achievable in the system, namely the PSR potential drop, the electric potential difference between the PSR and infinity ( $E_{\text{drop}} = e\sqrt{\dot{E}/c}$  with  $e$  the electron charge and  $c$  the speed of light). The possibility to accelerate particles up to such a high energy is a distinctive feature of old systems.

As discussed by Amato & Olmi (2021), the maximum achievable energy in a PWN is  $E_{\text{max}} = \min(E_{\text{drop}}, E_{\text{rad}})$ , where  $E_{\text{rad}} = 6 \text{ PeV } \eta^{1/2} B_{-4}^{1/2}$  is the maximum achievable energy for synchrotron-loss limited acceleration in an electric field equal to a fraction  $\eta \leq 1$  of the magnetic field in the acceleration region, and  $B_{-4}$  is the magnetic field in units of  $10^{-4}$  G. While the limit imposed by radiation losses is straightforward to understand, the appearance of  $E_{\text{drop}}$  might seem surprising if particle acceleration is not attributed directly to the PSR but rather to the TS. However, one can easily estimate the magnetic field  $B_{\text{TS}}$  at the TS position,  $R_{\text{TS}}$ , based on equilibrium between the ram-pressure of the flow upstream of the TS ( $\dot{E}/(4\pi c R_{\text{TS}}^2)$ ) and the downstream pressure, a fraction  $\xi \leq 1$  of which will be in the form of magnetic field. The result is  $B_{\text{TS}} =$

$\xi^{1/2} \sqrt{\dot{E}/c}/R_{\text{TS}}$ . It is then clear that the absolute maximum achievable energy, equal to the potential drop at the shock,  $\eta B_{\text{TS}} R_{\text{TS}}$ , equals  $E_{\text{drop}}$ , only achievable for  $\xi = \eta = 1$ .

In young systems, such as the Crab Nebula, the most stringent constraint on  $E_{\text{max}}$  comes from  $E_{\text{rad}}$ , given the high  $\dot{E}$  ( $> 10^{36}$  erg/s) and intense nebular field (100  $\mu\text{G}$  range). On the contrary, for evolved systems, with magnetic fields in the 1-10  $\mu\text{G}$  range, and  $10^{31} \leq \dot{E} \leq 10^{35}$  erg/s, the actual limit is  $E_{\text{drop}}$ . This is a solid argument to discriminate among the sources detected by LHAASO at EHE (Cao et al. 2021), those that can be associated with PSRs (López-Coto et al. in preparation). This is a needed step to clear the way for the detection of hadronic PeVatrons, the putative sources of the highest energy CRs in the Galaxy. PeV emission can either result from ICS of  $e^- - e^+$  with PeV energies scattering CMB photons in the Klein-Nishina regime, or from the decay of  $\pi^0$ s resulting from hadronic interactions of multi-PeV protons. Most sources in the Galaxy are not able to accelerate  $e^- - e^+$  to PeV energies, because acceleration would be limited to  $E_{\text{rad}}$  with  $\eta \approx (V/c) \ll 1$ , where  $V$  the typical flow speed in the acceleration region ( $V \approx c$  only for relativistic sources, meaning with relativistic temperature or bulk motion, or magnetically dominated). The only potential sources of PeV  $e^- - e^+$  are PSRs and their nebulae, and hence excluding them as the origin of the detected EHE emission strongly suggests that one is observing an actual hadronic PeVatron. A very interesting result in this sense is that the EHE source detected by LHAASO in Cygnus at energies up to 1.42 PeV cannot be associated with PSR J2032+4127 (López-Coto et al. in preparation). This strengthens the proposals that want the acceleration of PeV CRs associated with Star Forming Regions (Aharonian et al. 2019; Bykov et al. 2020) and massive star clusters (Morlino et al. 2021).

A peculiar aspect of the LHAASO detected PeVatrons is that most of them are rather extended sources (Cao et al. 2021), difficult to interpret as PWNe, but more likely associated with escaping particles. Detailed modeling is ongoing to derive constraints on the particle

transport and magnetic field in the emission region, and to make predictions of X-ray observability with instruments such as e-Rosita (López-Coto et al. in preparation).

### 3. The spectrum of CR leptons

There have been several attempts at reproducing the CR lepton spectrum including the contribution of PWNe (e.g. Blasi & Amato 2011; Bykov et al. 2017; Fornieri et al. 2020; Orusa et al. 2021, to mention a few). The main ingredients that determine the  $e^- - e^+$  spectrum at the Earth are: the  $e^- - e^+$  spectrum (total energy content and shape) injected in the ISM by the sources, the distribution of sources and diffusion coefficient in the Galaxy, the galactic magnetic and radiation field causing energy losses.

Evoli et al. (2020a) suggested how the latter could naturally explain the excess claimed by AMS-02 at energies  $\gtrsim 42$  GeV (Aguilar et al. 2019a): this feature could result from the transition to the Klein-Nishina regime of ICS on the UV radiation field. The treatment of ICS losses was refined in the work by Evoli et al. (2021), where a thorough calculation of the CR lepton spectrum at the Earth was performed using the most updated knowledge of all the relevant ingredients. The PSR population was built following the prescriptions of Faucher-Giguère & Kaspi (2006) for the initial PSR spin period and magnetic field (which determine the PSR total energy content and release history, and hence the requested efficiency of pair injection in the ISM). PSRs and SNRs were assumed to be born at the standard SN rate of 3 per century, and distributed through the Galaxy according to state-of-the-art models of the spiral structure. A Green function approach was used to compute the contribution at Earth of each source, adopting the diffusion coefficient that had been found by Evoli et al. (2020b) to best reproduce all available data on stable and unstable CR nuclei. The production of secondary  $e^- - e^+$  during propagation of protons was also taken into account. Fig. 1 shows the resulting  $e^+$  and all-lepton spectrum: it is clear that the proper inclusion of the PWN contribution (taking into account, in particular, a realistic dis-

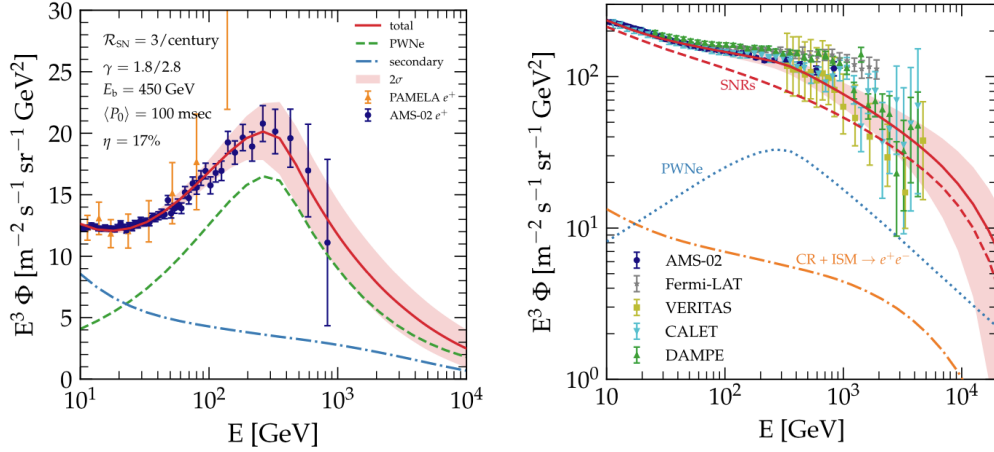


**Fig. 1.** The total spectrum of  $e^+$  (left panel) and  $e^- + e^+$  (right panel), compared to the available measurements. The different contributions and the chosen parameters are specified in the *legenda*. References for the data points can be found in Evoli et al. (2021) from which this figure is reproduced.

tribution of the source population in space and a realistic broken power-law spectrum) allows one to very well reproduce all the available CR lepton measurements.

This study led to a number of interesting results. Two of them are of particular relevance in the context of the present paper. First of all, the revised description of particle transport in the Galaxy following Evoli et al. (2020b) and the updated estimates of the fields determining radiation losses, causes the number of contributing sources at all energies to be much larger than found in previous studies: this number does decrease, as expected, with increasing energy, but keeps being as high as few hundreds PWNe and few tens of SNRs even for 10 TeV leptons. A direct consequence of this fact is that the chances for a local source to dominate the lepton flux at TeV energies is negligibly small, while it becomes non-negligible at energies  $\gtrsim 10$  TeV (Evoli et al. 2021). A second point concerns the spectrum of leptons that PWNe and SNRs are required to inject in the ISM: in both cases this is found to be steeper than expected.

The  $e^-$  spectrum injected by SNRs is found to have a power-law index  $\gamma_e = 2.6$ , steeper than the spectrum of protons by 0.3 ( $\gamma_p \approx 2.3$ ). A few attempts have been made in the liter-

ature to account for this difference. An obvious candidate is the effect of energy losses, that affect only leptons and might steepen their spectrum before release in the ISM, especially in the presence of largely amplified magnetic fields, as expected in SNR shocks as a result of streaming instabilities induced by the accelerated particles (Bell 2004; Amato & Blasi 2009). In fact, magnetic field amplification (MFA) due to CR streaming alone does not provide a large enough effect to explain the difference for  $e^-$  energies below  $10^2$ - $10^3$  TeV (Cristofari et al. 2021). However, as shown by Morlino & Celli (2021), the discrepancy between  $\gamma_e$  and  $\gamma_p$  can be explained assuming further MFA as a result of MHD type instabilities and a  $e^-$  acceleration efficiency inversely proportional to the shock speed and hence increasing with time during the SNR evolution.

In the case of PWNe the best fitting injection spectrum has  $\gamma_1 = 1.8$  and  $\gamma_2 = 2.8$  with a break at  $E_b = 450$  GeV. Comparing these values with the typical values mentioned in § 2, one soon realizes that, while  $\gamma_1$  and  $E_b$  are well in the range of observed values,  $\gamma_2$  is larger than typically observed in X-ray emitting PWNe (Reynolds et al. 2017). A possibility is that the observed sample is biased towards objects with a flatter spectrum, while an-

other interesting hypothesis is that some steepening of the released spectrum occurs in association with extended particle confinement around the sources.

#### 4. Particle escape from PWNe

The observation of extended halos of TeV emission around Geminga and Monogem (Abeysekara et al. 2017) was highly impactful. Modeling of these halos immediately suggested that they were the result of largely increased confinement times of  $e^-$  and  $e^+$  around these sources, implying in the region a diffusion coefficient  $\sim 100$  times smaller than the average value in the Galaxy. Understanding the processes by which these regions are formed, and assessing how widespread they are, is clearly very important: CR, both hadronic and leptonic, could in principle end up accumulating in these regions a non-negligible, and even dominant, fraction of the overall grammage associated with galactic propagation.

While several possible interpretations of this phenomenon have been put forward (see López-Coto et al. 2022 and references therein), an especially interesting possibility is that the observed halos are the result of the modifications induced in the ISM by the  $e^-$  and  $e^+$  leaving the source. Evoli et al. (2018) investigated the possibility that these particles guarantee their self-confinement by amplifying the level of magnetic fluctuations through the resonant streaming instability. This explanation was found to be viable only with a somewhat uncomfortable choice of the parameters. A more efficient way of amplifying magnetic turbulence is by means of the non-resonant branch of the streaming instability (Bell 2004), but this requires two conditions: 1) the presence of an electric current, not obvious if the streaming particles are  $e^- - e^+$  pairs; 2) that the energy density of streaming particles be larger than the ambient magnetic energy density.

The particle energy density in the source surrounding can be estimated from the detected  $\gamma$ -ray emission and is found to be  $\approx 10^{-2}$  eV/cm<sup>3</sup> (Giacinti et al. 2020). When compared with the energy density of the average magnetic field in the galactic disk ( $\approx 3$   $\mu$ G)

this would not be sufficient to excite the non-resonant streaming instability. However, deep X-ray studies of the Geminga region with XMM-Newton have failed to reveal the synchrotron emission that would be expected by the halo producing electrons in a  $3\mu$ G field and have allowed Liu et al. (2019) to set an upper limit on the local field:  $B < 1\mu$ G. The corresponding energy density is then less than  $2 \times 10^{-2}$  eV/cm<sup>3</sup>, which leaves open the possibility to excite the non-resonant streaming instability.

As for the existence of an electric current, this was indeed found, as a somewhat surprising result, in studies addressing the propagation of particles in and outside BSPWNe, in the field structure derived from 3D MHD simulations of these systems. Olmi & Bucciantini (2019b) performed an extended numerical study of BSPWNe with the PLUTO code (Mignone et al. 2007, 2012). They found that the escape of particles from BSPWNe is strongly energy dependent. Low energy particles are only free to escape from the BSPWN tail, but particles above a threshold energy, of order 30% of  $E_{\text{drop}}$ , can effectively escape from the bow-shock head. Particles injected in different sectors of the PSR wind TS form currents that, depending on the level of turbulence in the bow shock tail (see Olmi & Bucciantini 2019a), can survive in the nebular plasma and reach the bow shock boundary, from which they escape in the ISM. In Fig. 2 we show the release of  $e^-$  and  $e^+$  of different energies: lower energy particles tend to escape in jets, while particles close to  $E_{\text{drop}}$  escape almost isotropically. In addition, the flow is charge separated at the 1-10% level, depending on the conditions in the nebula (magnetization of the flow, level of anisotropy of the wind – Olmi & Bucciantini 2019a). For such level of charge separation, depending on the magnetic field strength in the ISM around the source, it is well possible that the non-resonant streaming instability is excited and gives rise to the needed level of turbulence to explain the observed suppression of the diffusion coefficient.

The difference between the spherical halos observed around Geminga and Monogem, and the misaligned X-ray jets associated to other

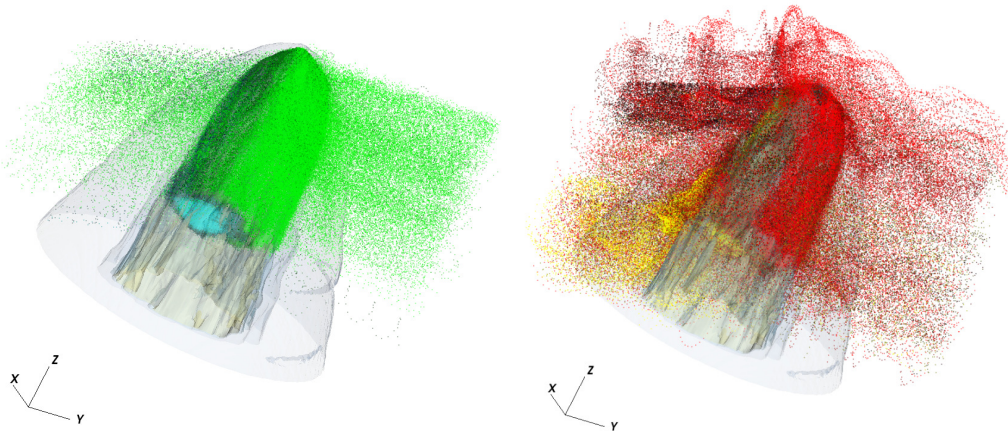


**Fig. 2.** 3D maps of the bow shock, shown in grey, and particles escaping from the system (from Olmi & Bucciantini (2020)). *Left panel:* electrons with  $E = 30\%E_{\text{drop}}$ , with different colors indicating different injection locations along the TS (green:  $0^\circ - 60^\circ$ ; black:  $60^\circ - 120^\circ$ ; cyan:  $120 - 180^\circ$ ; angle measured from the direction of the PSR proper motion). *Right panel:* positrons of energy  $90\%E_{\text{drop}}$  (red:  $0^\circ - 60^\circ$ ; black:  $60^\circ - 120^\circ$ ; yellow:  $120 - 180^\circ$ ). For additional details see Olmi & Bucciantini (2019b).

BSPWNe might be a result of the different ambient magnetic field strength (less than  $1\mu\text{G}$  around sources showing halos, tens of  $\mu\text{G}$  in the case of jets). A careful study of the parameter space and a quantitative assessment of the level of charge separation of the escaping particle currents are ongoing, in order to estimate the likelihood of halo formation (Olmi et al in preparation) and the implications on CR transport in the Galaxy.

## 5. Conclusions

In this article we have summarized recent and ongoing work on CR  $e^-$  and  $e^+$ , showing how the spectrum measured at the Earth for both species can be very well reproduced by models including the contribution of PWNe. These models require the sources of CR leptons to inject a steeper than expected spectrum and discussed how this fact requires MFA in the case of SNRs and might depend on unsettled, possibly non-linear, aspects of the particle escape in the case of PWNe.

Observations, in the X-rays and at VHE and EHE, are unveiling increasing complex-

ity. We suggest a scenario in which the escape of particles from evolved PWNe is governed by the amplification of magnetic turbulence induced by the same particles leaving the source. The branches of instability that the particles can excite strongly depend on the local ISM magnetic field, on the flux of particles and on the associated electric current, with the latter two ingredients depending on the PWN structure and ultimately on the PSR wind properties in terms of anisotropy and magnetization. A quantitative assessment of these ideas will come from the combination of additional high energy observations and further theoretical efforts, both numerical (MHD + particle transport) and semi-analytical.

*Acknowledgements.* All authors acknowledge support and fundings from Accordo Attuativo ASI-INAF n. 2017-14-H.0.

## References

- Abeysekara, A. U., Albert, A., Alfaro, R., et al. 2017, *Science*, 358, 911
- Adriani, O., Barbarino, G. C., Bazilevskaia, G. A., et al. 2009, *Nature*, 458, 607

- Aguilar, M., Alberti, G., Alpat, B., et al. 2013, *Phys. Rev. Lett.*, 110, 141102
- Aguilar, M., Ali Cavasonza, L., Alpat, B., et al. 2019a, *Phys. Rev. Lett.*, 122, 101101
- Aguilar, M., Ali Cavasonza, L., Ambrosi, G., et al. 2019b, *Phys. Rev. Lett.*, 122, 041102
- Aharonian, F., Yang, R., & de Oña Wilhelmi, E. 2019, *Nature Astronomy*, 3, 561
- Amato, E. 2019, in *High Energy Phenomena in Relativistic Outflows VII*, 33
- Amato, E. & Blasi, P. 2009, *MNRAS*, 392, 1591
- Amato, E. & Blasi, P. 2018, *Advances in Space Research*, 62, 2731
- Amato, E. & Casanova, S. 2021, *Journal of Plasma Physics*, 87, 845870101
- Amato, E. & Olmi, B. 2021, *Universe*, 7, 448
- Bandiera, R. 2008, *A&A*, 490, L3
- Bandiera, R., Bucciantini, N., Martín, J., Olmi, B., & Torres, D. F. 2020, *MNRAS*, 499, 2051
- Bell, A. R. 2004, *MNRAS*, 353, 550
- Blasi, P. & Amato, E. 2011, in *Astrophysics and Space Science Proceedings*, Vol. 21, *High-Energy Emission from Pulsars and their Systems*, 624
- Bykov, A. M., Amato, E., Petrov, A. E., Krassilchtchikov, A. M., & Levenfish, K. P. 2017, *Space Sci. Rev.*, 207, 235
- Bykov, A. M., Marcowith, A., Amato, E., et al. 2020, *Space Sci. Rev.*, 216, 42
- Cao, Z., Aharonian, F. A., An, Q., et al. 2021, *Nature*, 594, 33
- Cristofari, P., Blasi, P., & Caprioli, D. 2021, *A&A*, 650, A62
- de Vries, M. & Romani, R. W. 2020, *ApJ*, 896, L7
- Evoli, C., Amato, E., Blasi, P., & Aloisio, R. 2021, *Phys. Rev. D*, 103, 083010
- Evoli, C., Amato, E., Blasi, P., & Aloisio, R. 2021, *Phys. Rev. D*, 104, 123029
- Evoli, C., Blasi, P., Amato, E., & Aloisio, R. 2020a, *Phys. Rev. Lett.*, 125, 051101
- Evoli, C., Linden, T., & Morlino, G. 2018, *Phys. Rev. D*, 98, 063017
- Evoli, C., Morlino, G., Blasi, P., & Aloisio, R. 2020b, *Phys. Rev. D*, 101, 023013
- Faucher-Giguère, C.-A. & Kaspi, V. M. 2006, *ApJ*, 643, 332
- Fiori, M., Olmi, B., Amato, E., et al. 2022, *MNRAS*, 511, 1439
- Fornieri, O., Gaggero, D., & Grasso, D. 2020, *JCAP*, 2020, 009
- Giacinti, G., Mitchell, A. M. W., López-Coto, R., et al. 2020, *A&A*, 636, A113
- Hui, C. Y. & Becker, W. 2007, *A&A*, 467, 1209
- Kargaltsev, O., Pavlov, G. G., Klingler, N., & Rangelov, B. 2017, *Journal of Plasma Physics*, 83, 635830501
- Kim, S. I., Hui, C. Y., Lee, J., et al. 2020, *A&A*, 637, L7
- Klingler, N., Rangelov, B., Kargaltsev, O., et al. 2016, *ApJ*, 833, 253
- Klingler, N., Yang, H., Hare, J., et al. 2020, *arXiv e-prints*, arXiv:2008.09200
- Liu, R.-Y., Ge, C., Sun, X.-N., & Wang, X.-Y. 2019, *ApJ*, 875, 149
- López-Coto, R., de Oña Wilhelmi, E., Aharonian, F., Amato, E., & Hinton, J. 2022, *Nature Astronomy*, 6, 199
- López-Coto, R., de Oña Wilhelmi, E., Amato, E., & Aharonian, F. in preparation
- Mignone, A., Bodo, G., Massaglia, S., et al. 2007, *ApJS*, 170, 228
- Mignone, A., Zanni, C., Tzeferacos, P., et al. 2012, *ApJS*, 198, 7
- Morlino, G., Blasi, P., Peretti, E., & Cristofari, P. 2021, *MNRAS*, 504, 6096
- Morlino, G. & Celli, S. 2021, *MNRAS*, 508, 6142
- Olmi, B. & Bucciantini, N. 2019a, *MNRAS*, 484, 5755
- Olmi, B. & Bucciantini, N. 2019b, *MNRAS*, 490, 3608
- Olmi, B. & Bucciantini, N. 2020, *Mem. Soc. Astron. Italiana*, 91, 321
- Orusa, L., Manconi, S., Donato, F., & Di Mauro, M. 2021, *JCAP*, 2021, 014
- Pavan, L., Bordas, P., Pühlhofer, G., et al. 2014, *A&A*, 562, A122
- Reynolds, S. P., Pavlov, G. G., Kargaltsev, O., et al. 2017, *Space Sci. Rev.*, 207, 175
- Serpico, P. D. 2012, *Astropart. Phys.*, 39, 2
- Temim, T., Slane, P., Kolb, C., et al. 2015, *ApJ*, 808, 100
- Torres, D. F., Lin, T., & Coti Zelati, F. 2019, *MNRAS*, 486, 1019